Precision & Performance Conference 2025, Cranfield University, UK, 17th- 20th November 2025

Characterisation of the Cyclic Errors During Linear Motion of an Articulated Robot

Khin Khant, Simon Fletcher, Andrew Longstaff, Ashley Cusack, and Andrew Bell

Centre for Precision Technologies, University of Huddersfield, United Kingdom

Khinwin.Khant@hud.ac.uk

Abstract

Industrial robots are increasingly being considered for adoption in machining operations due to their cost-effectiveness, larger workspace, and operational flexibility compared to conventional CNC machines. However, intrinsic cyclic errors arising from gearbox pitch variations, encoder interpolation limitations, and structural compliance effects can limit the achievable accuracy and surface quality in precision machining applications. This study presents a method for the characterisation of cyclic errors of an industrial articulated robot using a Renishaw XM-60 laser in continuous capture mode. The approach does not seek to detect the root-cause of the errors, but rather to identify what effects are likely to be seen if commanded to make a linear motion when machining. The results from the laser were compared with analysis of the surface of a machined test block using a coordinate measuring machine (CMM).

The investigation showed that this method could detect the cyclic errors, whose frequency was shown to match the defects in the surface generated by machining. As anticipated, the absolute magnitude of the cyclic error differs between no-load laser measurements and surface of the machined block due to effects by additional factors such as cutting forces, tools behaviours and vibrations. This suggests that the robot's intrinsic structural and control system characteristics are a major contributor to the cyclic error behaviour, which are then further amplified by machining forces during cutting and compounded by tool-pass frequencies. Further work is required to establish a method to link the amplitude from laser results to magnitude of error under machining conditions. Notably, the laser revealed a directional dependency, which could be used to improve machining performance through changes in toolpath-planning.

The methodology presented enables robust characterisation of cyclic errors, providing a foundation for developing targeted compensation strategies to enhance dimensional accuracy and surface finish in robotic machining applications.

Keywords

Robotic machining, cyclic error, CMM, XM-60, interpolation error, vibration, geometric calibration, surface quality.

1. Introduction

The adoption of industrial robots for precision machining tasks, such as drilling, milling, and cutting, has grown rapidly in recent years, driven by the need for flexible automation and cost reduction in manufacturing [1]. Unlike traditional CNC machines, robots can offer a larger working envelope for their given footprint and can be readily reconfigured for different tasks, making them attractive for industries handling large or complex components. However, the transition from conventional machine tools to robotic machining introduces new challenges, particularly in maintaining high levels of accuracy and repeatability. One possible issue is the presence of cyclic errors during linear motion, which can compromise both the dimensional precision and surface integrity of machined parts. These errors, often linked to the robot's mechanical transmission, encoder resolution, and control algorithms, present a significant barrier to the wider use of robots in high-precision applications.

2. Literature Review and Research Gap

While offline error compensation and robot calibration have been extensively studied, cyclic errors during real-world machining operations remain insufficiently explored, especially under the influence of cutting forces and dynamic excitation. Most researchers have focused on static positioning accuracy and geometric calibration, with limited attention paid to cyclic errors that arise during continuous machining processes. While the pose accuracy of a robot end-effector directly influences surface quality and process performance [2], geometric errors have been identified as the dominant source of inaccuracy in industrial robots [3].

However, interpolation errors caused by path discretisation and trajectory inaccuracies are typically measured using different sensors [4], and result from planning strategies within robot controllers. These lead to deviations between the commanded and actual end-effector paths, particularly in redundant manipulators with multiple inverse kinematics solutions [5].

The inverse kinematics problem is inherently more complex than forward kinematics due to its nonlinear nature and the existence of multiple possible solutions. These are typically solved using either analytical or numerical methods, with the latter more commonly applied [6].

Previous studies have proposed spatial interpolation-based compensation methods, such as neural networks [7], [8], to estimate and correct pose errors at unmeasured locations. Despite their promise, these approaches predominantly address static or quasi-static errors, and their applicability is constrained in tasks involving frequent orientation changes or complex toolpaths due to the curse of dimensionality in joint space sampling [9], [10]. Moreover, such compensation methods do

not directly evaluate dynamic interpolation errors, which manifest as cyclic deviations during continuous tool motion.

In this context, the present study addresses this gap by measuring cyclic errors from robot linear motion trajectories using a continuous laser multi axis calibrator XM-60 and comparing them with surface straightness errors measured on the edges of machined aluminium cubes using a CMM. By correlating the cyclic errors observed in robot motion with those appearing on the machined workpiece, this integrated methodology characterises the robot's interpolation-induced cyclic error characteristics under practical machining conditions, thereby providing insights to support toolpath optimisation and improve compensation strategies for enhanced robotic machining accuracy.

3. Methodology

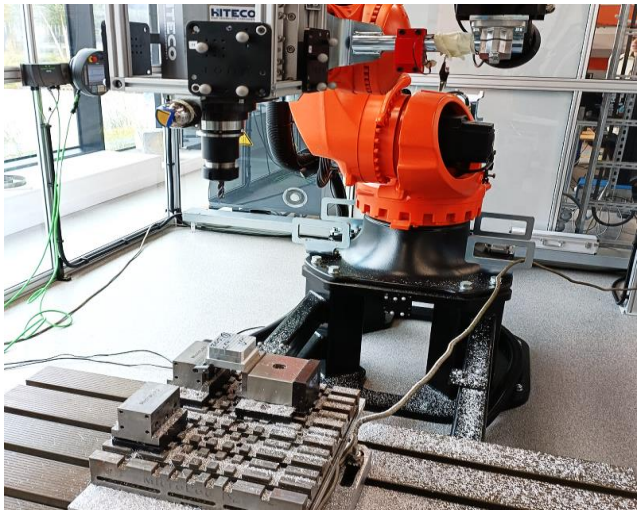

Fig. 1: Machining an aluminium cube with Kuka KR210

A measurement methodology was implemented on a 6-axis KUKA KR210 industrial robot equipped with a milling spindle to investigate the characteristics of cyclic errors during block cutting operations (**Fig. 1**). The approach combined high-precision surface analysis using a ZEISS Coordinate Measuring Machine (CMM) (**Fig. 2**), and continuous linear axis error measurement using a Renishaw XM-60 multi axis laser calibrator (**Fig. 3**).

Fig. 2: Measuring with Coordinate Measuring Machine (CMM)

The XM-60 was mounted on the robot's flange to capture all six degrees of freedom (6DoF) during X± traverses at a feedrate of 1275 mm/min under no-load conditions in three paths of Y axis: positive, centre, and negative sides, corresponding to the position of rear, centre, and front of the machined block, as illustrated in (**Fig. 4**).

To isolate cyclic errors, the linear slope was removed using a least-squares fit, and frequency analysis was then performed using Fast Fourier Transform (FFT). Finally, the cyclic error magnitude was quantified using the difference of peak-to-peak metric.

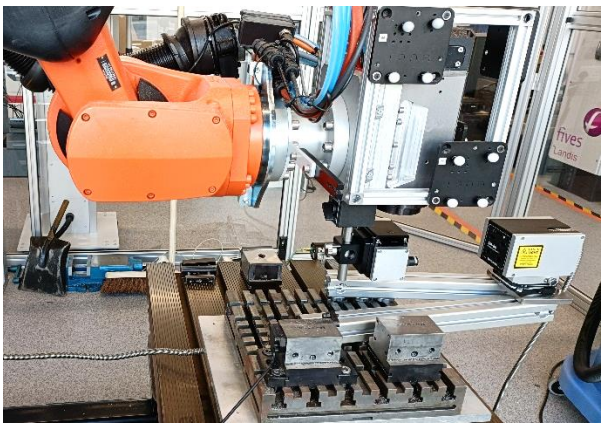

Fig. 3: Continuous linear motion calibration of Kuka KR210 with Renishaw XM-60

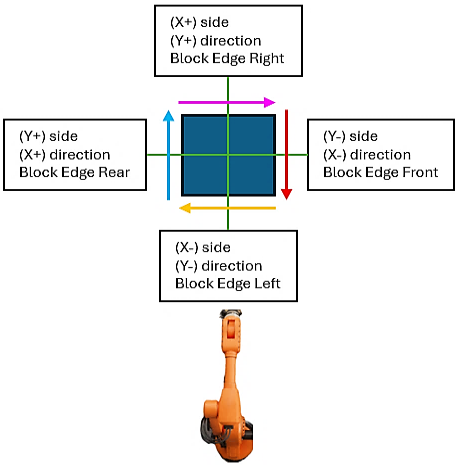

Fig. 4: XM-60 calibration directions

4. Results and Discussion

4.1 CMM Results and Discussion

4.1.1 CMM Result of Block Finish Cut

The surface measurement results obtained from the Coordinate Measuring Machine (CMM) (**Fig. 2**) showed clear evidence of periodic geometric deviations on all four edges of the machined parts on both rough and finish cuts. The corresponding results are presented in the CMM finish cut results (**Table 1**).

Table 1: CMM Finish Cut Results

Direction	(X+) dir (Edge rear top)	(X-) dir (Edge front top)	(Y-) dir (Edge right top)	(Y+) dir (Edge left top)
Number of peaks within 46mm distance cut	2	7	5	5
Cyclic error (um)	33	49	60	72

In the (X-) direction (Edge Front Top), the measured cyclic error was 49 µm 7 peaks (**Fig. 5**), and for the (X+) direction (Edge Rear Top), the cyclic error was 33 µm 2 peaks (**Fig. 6**). Notably, the edges aligned with the Y axis exhibited greater cyclic deviations: 60 µm for (Y-) and 72 µm for (Y+), both showing a similar peak number (**Fig. 7**), (**Fig. 8**).

These CMM results demonstrate that the machining process retains evidence of robot-induced cyclic motion, although the magnitude of these errors appears to be attenuated, likely due to the material removal process and structural damping effects.

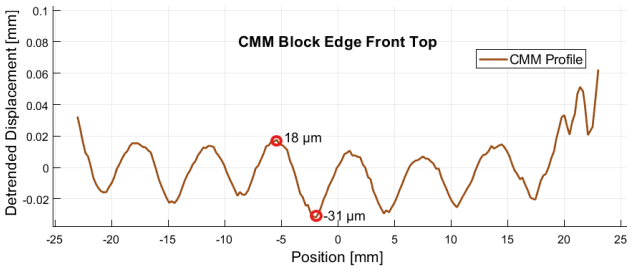

Fig. 5: Edge front top (X-) direction cut CMM result (finish cut)

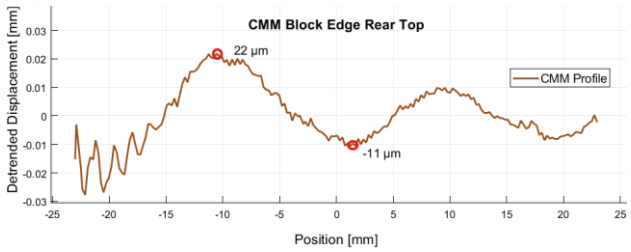

Fig. 6: Edge rear top (X+) direction cut CMM result (finish cut)

Fig. 7: Edge right top (Y-) direction cut CMM result (finish cut)

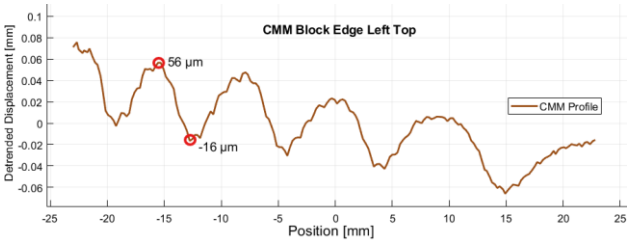

Fig. 8: Edge left top (Y+) direction cut CMM result (finish cut)

4.2 XM60 Results and Discussion

The continuous X axis linear motion measurements results captured by using the Renishaw XM-60 multi axis laser calibrator (**Fig. 3**) showed consistently cyclic error of forward and reverse both directions. Although all 6DoF data were acquired, horizontal straightness was the most sensitive to the cutting process and is therefore presented here.

XM-60 measurement results data within region of interest (ROI) 46mm, same position of block cut, are summarised in (**Table 2**).

Table 2*:* XM-60 Measurement Results

	1275 mm/min (Y+) side		1275 mm/min (Centre)		1275 mm/min (Y-) side	
Direction	(X+) dir, reverse	(X-) dir, forward	(X+) dir, reverse	(X-) dir, forward	(X+) dir, reverse	(X-) dir, forward
Number of constant velocity peaks within 46 mm distance ROI	2	2	5	5	7	7
Cyclic error (um)	47	47	43	43	58	58

4.2.1 XM60 (Y+) side X axis continuous linear movement at feedrate 1275 mm/min no load condition

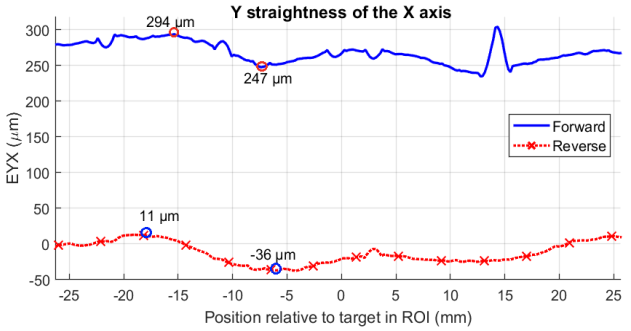

Fig. 9: Y straightness of the X axis in ROI (Y+ side)

4.2.2 XM60 (Centre) side X axis linear movement at feedrate 1275 mm/min no load condition

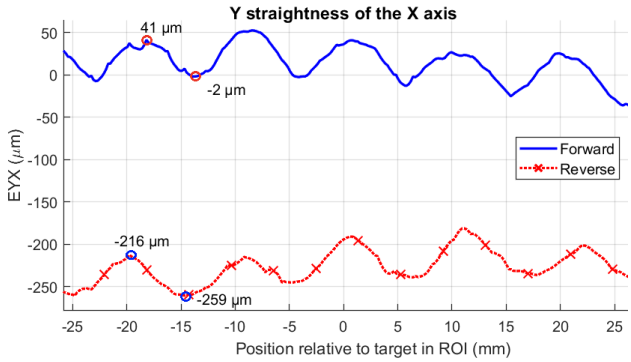

Fig. 10: Y straightness of the X axis in ROI (centre)

4.2.3 XM60 (Y-) side X axis linear movement at feedrate 1275 mm/min no load condition

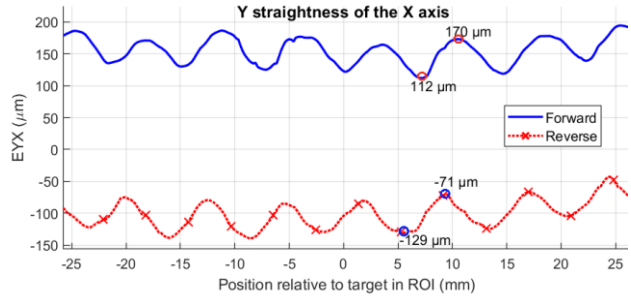

Fig. 11: Y straightness of the X axis in ROI (Y- side)

On the (Y+) side, both (X-) forward and (X+) reverse directions showed identical cyclic error of 47 µm and 2 peaks (**Fig. 9**), measured within ROI 46mm of machined block cut position, which corresponds to the edge rear top in the CMM scan. At the centre, cyclic errors slightly decrease to 43 µm with increasing errors 5 peaks in both directions (**Fig. 10**), indicating a bit lower excitation or joint influence at mid-span. On the (Y-) side, the (X-) forward and (X+) reverse directions again exhibited matching values of 58 µm with the highest peak count of 7 (**Fig. 11**), also aligned with the edge front top of the machined block.

These results confirm strong forward/reverse symmetry in each path, with consistent peak numbers and amplitudes. However, the variation across (Y+) to (Y-) sides and the central path indicates clear directional and positional dependency. Specifically, the increasing number of peaks from 2 in the (Y+) side, to 5 in the centre, and 7 in the (Y-) side suggests a rising spatial frequency of cyclic deviations as the tool moves from rear to front. This suggests that underlying joint kinematics and structural dynamics may contribute to cyclic behaviour and should be further investigated to support more effective compensation strategies.

4.3 XM60 and CMM Combined Discussion

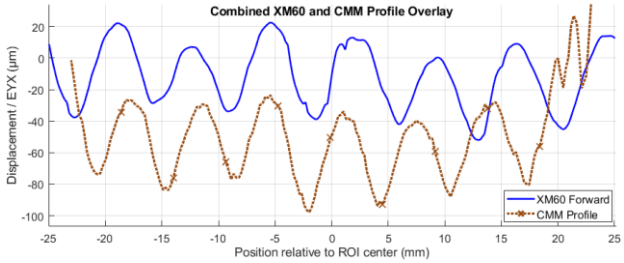

Fig. 12: Y straightness error of the X axis (XM-60 (X-) direction (Y-) side (blue) and CMM edge front top cyclic error (black))

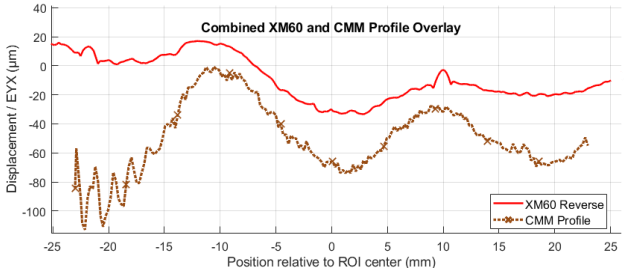

Fig. 13: Y straightness error of the X axis (XM-60 (X+) direction (Y+) side (blue) and CMM edge rear top cyclic error (black))

The overlay plots in (**Fig. 12**) and (**Fig. 13**) demonstrate a strong correspondence between the cyclic errors measured using the XM-60 laser and those observed on the machined surface via CMM. For both the XM-60 (X-) direction on the (Y-) side (corresponding to the CMM front top edge) and the (X+) direction on the (Y+) side (CMM rear top edge), the number of peaks and overall waveform shape closely match across both measurement methods, even though their amplitudes differ due to cutting-related damping and material interaction. The slight phase misalignment between the signals likely results from the machining process acting as a low-pass filter, which smooths and shifts the imprint of motion-induced errors. Additional contributing factors may include tool deflection, dynamic cutting responses, or slight discrepancies in reference alignment between the two measurement systems.

4.4 FFT Spectrum Comparison

Even though the CMM amplitude has been scaled 500 × to make its frequency structure visible on the same axis with XM-60 amplitude, both spectra exhibit prominent peaks at 0.14~0.15 cycles/mm, confirming that the dominant cyclic components from robot motion are also present on the machined surface very closely alignment (**Fig. 14**).

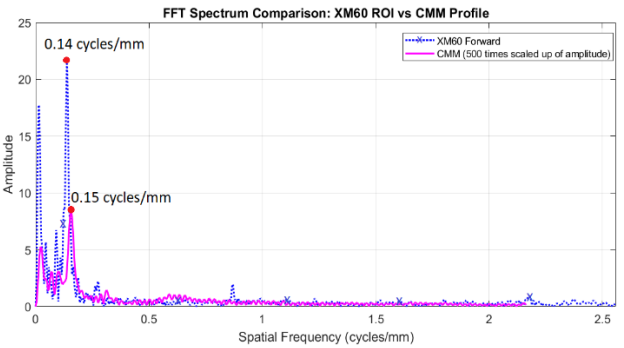

Fig. 14: Y straightness error of X axis FFT spectrum at (X-) direction (Y-) side in ROI 46mm length of machined block position (blue) vs CMM block edge front cut FFT spectrum (pink)

However, it is critical to note that FFT analysis is not reliable characterise surface quality or judge cyclic behaviour in machining contexts. While FFT effectively highlights periodic components, the cyclic error of the machined part is not only due to motion of robot, but also from due to from tool deflection, spindle vibration, material damping, or process-induced noise. Furthermore, CMM data captured after tool-material interaction naturally acts as a low-pass filter, reducing high-frequency content and suppressing certain error signatures that were clearly visible in the XM-60 signal.

5. Conclusion

This study demonstrated a method to characterise cyclic errors during robot linear motion by combining Renishaw XM-60 dynamic measurements and CMM surface inspections. The results revealed that the number of cyclic peaks identified on the machined surfaces closely matched those observed in the dynamic XM-60 measurements, confirming a direct correlation between robot motion and surface error patterns. Although the amplitude of errors differed due to machining influences such as cutting forces and damping, the spatial frequency and waveform remained consistent. Importantly, this highlights that surface deviations are primarily induced by the robot's motion characteristics.

Acknowledgment

The authors would like to acknowledge the support from the EPSRC The Future Advanced Metrology Hub for Sustainable Manufacturing (Ref. EP/Z53285X/1) and UKRI Advanced Machinery & Productivity Initiative (Ref. 84646) for the funding for this work.

References

[1] Kromoser B, Pantscharowitsch M, & Witzeneder J 2023. Increasing efficiency of an industrial robot when machining timber beams – introduction of a parametric solving model to determine optimised stacks. *Wood Material Science and Engineering*. **18** (5), 1724–1740.

[2] Le M, Patrick B, Patrick MS, Robert GL, Douglas AB 2018. Modeling and calibration of high-order joint-dependent kinematic errors for industrial robots. *Robotics and Computer-Integrated Manufacturing*. Vol. **50**.

[3] Min H, Xiaoqi T, Zhouxiang J, Yixuan G 2021. A new calibration method for joint-dependent geometric errors of industrial robot based on multiple identification spaces. *Robotics and Computer-Integrated Manufacturing*. Volume **71**.

[4] Pivarčiová E, Božek P, Turygin Y 2018. Analysis of control and correction options of mobile robot trajectory by an inertial navigation system. *International Journal of Advanced Robotic Systems*. **15** (1).

[5] Cheng Q, Cao S, Guo Y, Zhu W, Wang H and Ke Y 2022. Pose error compensation based on joint space division for 6-DOF robot manipulators. *Precision Engineering.* Vol. **74***.*

[6] Chen, Y, Luo X, Han B, Jia Y, Liang G, & Wang X 2019. A General Approach Based on Newton's Method and Cyclic Coordinate Descent Method for Solving the Inverse Kinematics. *Applied Sciences*. ***9***(24), 5461.

[7] Cao CT, Do VP, Lee BR 2019. A Novel Indirect Calibration Approach for Robot Positioning Error Compensation Based on Neural Network and Hand-Eye Vision. *Applied Sciences*. **9** (9):1940.

[8] Yuxiang W, Hongfei Z, Xiang Z, Chentao M ,and Zhirong W 2020. Improvement of Heavy Load Robot Positioning Accuracy by Combining a Model-Based Identification for Geometric Parameters and an Optimized Neural Network for the Compensation of Nongeometric Errors. *Wiley*. 5896813.

[9] Yuanfan Z, Wei T, Wenhe L 2016. Positional error similarity analysis for error compensation of industrial robots. *Robotics and Computer-Integrated Manufacturing*. Volume **42**.

[10] Yin G, Shibin Y, Yongjie R, Jigui Z, Shourui Y, Shenghua Y 2015. A multilevel calibration technique for an industrial robot with parallelogram mechanism, *Precision Engineering*. Volume **40**.